

# Electrochemical Polymerization of Acrylics on Stainless Steel Cathodes

S. L. Cram,<sup>1,2</sup> G. M. Spinks,<sup>1,2</sup> G. G. Wallace,<sup>1</sup> H. R. Brown<sup>2</sup>

<sup>1</sup>Intelligent Polymer Research Institute, University of Wollongong, Northfields Avenue, Wollongong, New South Wales 2522, Australia

<sup>2</sup>Institute for Steel Processing and Products, University of Wollongong, Northfields Avenue, Wollongong, New South Wales 2522, Australia

Received 27 August 2001; accepted 29 April 2002

**ABSTRACT:** A cathodic, aqueous-based technique for producing uniform, thin, passive films of poly(methyl methacrylate) and poly(glycidylacrylate) on stainless steel electrodes was developed. The films were chemically characterized by Fourier transform infrared spectroscopy, NMR spectroscopy, and differential scanning calorimetry. The thickness (quantified by ellipsometry) and morphology of

the films were dependent on the electrolysis time and potential and were also influenced by the individual monomer properties. © 2002 Wiley Periodicals, Inc. *J Appl Polym Sci* 87: 765–773, 2003

**Key words:** thin films; electron microscopy; FT-IR; morphology

## INTRODUCTION

Electrochemical polymerization (ECP) is a technique that has been widely developed to produce conducting polymer films that are synthesized for specialized applications such as microelectronics, photo-electrochemistry, electrocatalysis, or energy storage.<sup>1</sup> This technique is also ideal for forming thin, passive films on electrodes and is suitable for applications such as corrosion protection and adhesion enhancement. Indeed, there are a number of publications in the literature that describe the use of insulating or electroactive electropolymerized films on metal surfaces for corrosion protection.<sup>2–7</sup> The use of ECP to produce nonconducting films for enhanced adhesion applications in the carbon fiber composite industry has also received notable attention.<sup>8–14</sup> However, the use of ECP to produce insulating films as adhesion-promoting pretreatments on metals is still relatively unexplored.

ECP processes offer the advantage of synthesizing polymeric films *in situ* from monomeric starting materials, thereby eliminating many of the processing steps associated with the manufacture and application of paints or primers. The development of ECP in the coatings arena, therefore, offers potential economical and practical advantages.

Although there have been numerous fundamental studies of ECP methods to form nonconducting coatings on metallic electrodes, many of these studies have been based on phenolic monomers or organic solvents, which raise environmental and/or health issues limiting the large scale use of such a processes. Also, many of the techniques described have been based on electro-oxidative polymerizations at the anode. At metallic electrodes, it would be preferable to avoid such methods so as to prevent oxidation of the metal during the process. Therefore, this study was restricted to the production of thin, passive, polymeric films on metallic electrodes from aqueous electrolytes by the use of electroreductive methods.

To achieve the aim described, methyl methacrylate (MMA) and glycidyl acrylate (GA) were electropolymerized in dilute, aqueous sulfuric acid systems containing potassium persulphate to form passive coatings on stainless steel cathodes. MMA was chosen because it has previously been shown to undergo electroreductive polymerization (ERP) in sulfuric acid electrolytes to form coatings on carbon<sup>11</sup> and because of its carbonyl functionality, which would be expected to form secondary bonds with metallic oxides. GA has also been previously shown to undergo ERP in aqueous sulfuric acid solutions to form coatings on graphite fibre electrodes.<sup>13–15</sup> The combination of epoxide and acrylic functionalities in the GA monomer accounts for a simultaneous increase in impact and interlaminar shear strengths of composites made from these pretreated carbon fibers<sup>13,14</sup> when used with an epoxy matrix.

Correspondence to: G. M. Spinks (geoff\_spinks@uow.edu.au).

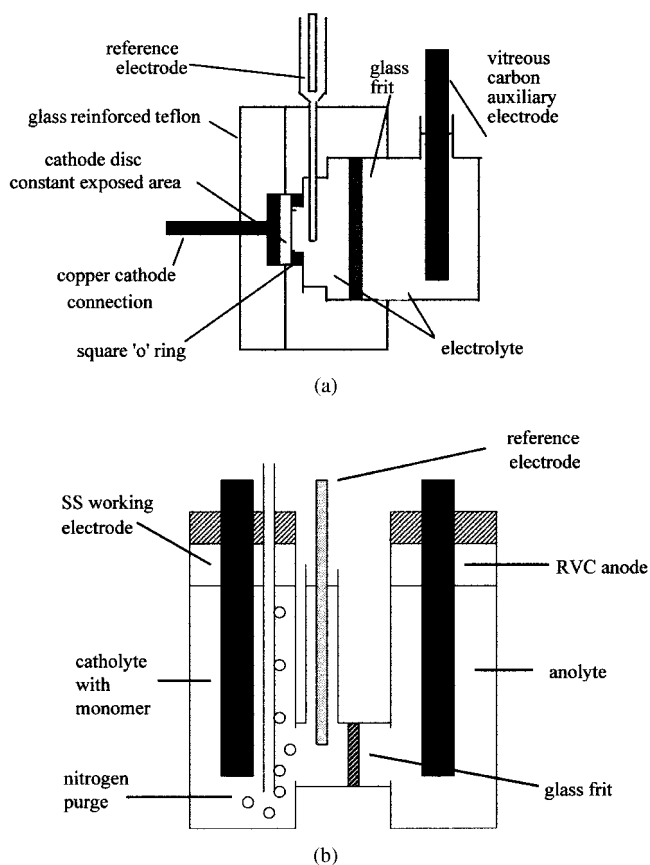


**Figure 1** (a) Standard electropolymerization cell and (b) H-cell used for making larger coating samples.

A detailed study of the ERP of MMA or GA on metallic cathodes from aqueous solutions has not previously been reported, and the aim of this study was to demonstrate the possibility of this synthesis and to establish the optimum coating conditions. The polymerization mechanism and adhesion-enhancing performance of these films will be described in forthcoming publications.

## EXPERIMENTAL

### Materials and preparation

We purified MMA monomer (Sigma Aldrich, Sydney, Australia) by washing it with 5% sodium hydroxide three times and then rinsing it with distilled water four times. The monomer was stored in a refrigerator over sodium sulfate and was used within 14 days. All other chemicals, including GA monomer (Polysciences, Warrington, PA), were used as supplied without further purification.

Stainless steel working electrodes, austenitic grade 316, were prepared from a 0.7 mm thick sheet and polished flat to a 1- $\mu$ m finish. Before electrolysis, each electrode was wiped with ethanol and cleaned for 10 min in an Ultra Violet Ozone Cleaning System

(UVOCS Inc., Montgomeryville, PA). Reticulated vitreous carbon (RVC; Energy Research and Generation Inc., Oakland, CA) was cut to size and used as the anode in all electrochemical experiments without further modification.

### Electropolymerization

Two electrochemical cells were used for potentiostatic coating experiments. The standard coating cell is shown in Figure 1(a), and the H-cell, with larger stainless steel cathodes, is shown in Figure 1(b). Both cells were divided into cathodic and anodic compartments by a glass frit of medium porosity. In the standard cell, the working electrodes were clamped into the cathode side of the cell, exposing a constant area of 5.725 cm<sup>2</sup>, by means of an O-ring. In the H-cell, the working electrodes were rectangular plates with a constant exposed area of 13.75 cm<sup>2</sup>. The Ag/AgCl reference electrode was secured in close proximity to the working electrodes by a Luggin's capillary. The constant volume RVC auxiliary electrode was secured in the anode side of the cell.

The standard cell was used to produce coatings under various electrochemical and solution conditions, whereas the H-cell was used to produce the larger polymer samples required for various characterization techniques. Analysis of samples produced in the H-cell was carried out after the physical removal of the coatings from the electrode.

### Electropolymerization procedure

Electropolymerizations were carried out at room temperature. Dilute acid (0.025M H<sub>2</sub>SO<sub>4</sub>) was added to both sides of the cell to be used, whereas 0.1M monomer, MMA or GA, and 0.01M potassium persulphate (K<sub>2</sub>S<sub>2</sub>O<sub>8</sub>) were added to the catholyte only. The catholyte was purged with nitrogen for 10 min before any potential was applied. The potential was then ramped at 2 mV/s from 0 V (vs. Ag/AgCl) to the

**TABLE I**  
Electropolymerization Conditions: Various Electrolysis Times and Potentials

Potential (V)	Hold time (min)					
	2.5	5.0	7.5	10.0	15.0	30.0
-0.2					✓*	
-0.3	✓*	✓*	✓*	✓*	✓*	
-0.4	✓	✓	✓	✓	✓*	✓
-0.5					✓*	
-0.6					✓*	
-0.7					✓*	

✓ indicates that the coatings were made in 0.1M MMA solutions. \* indicates that the coatings were made in 0.1M GA solutions.

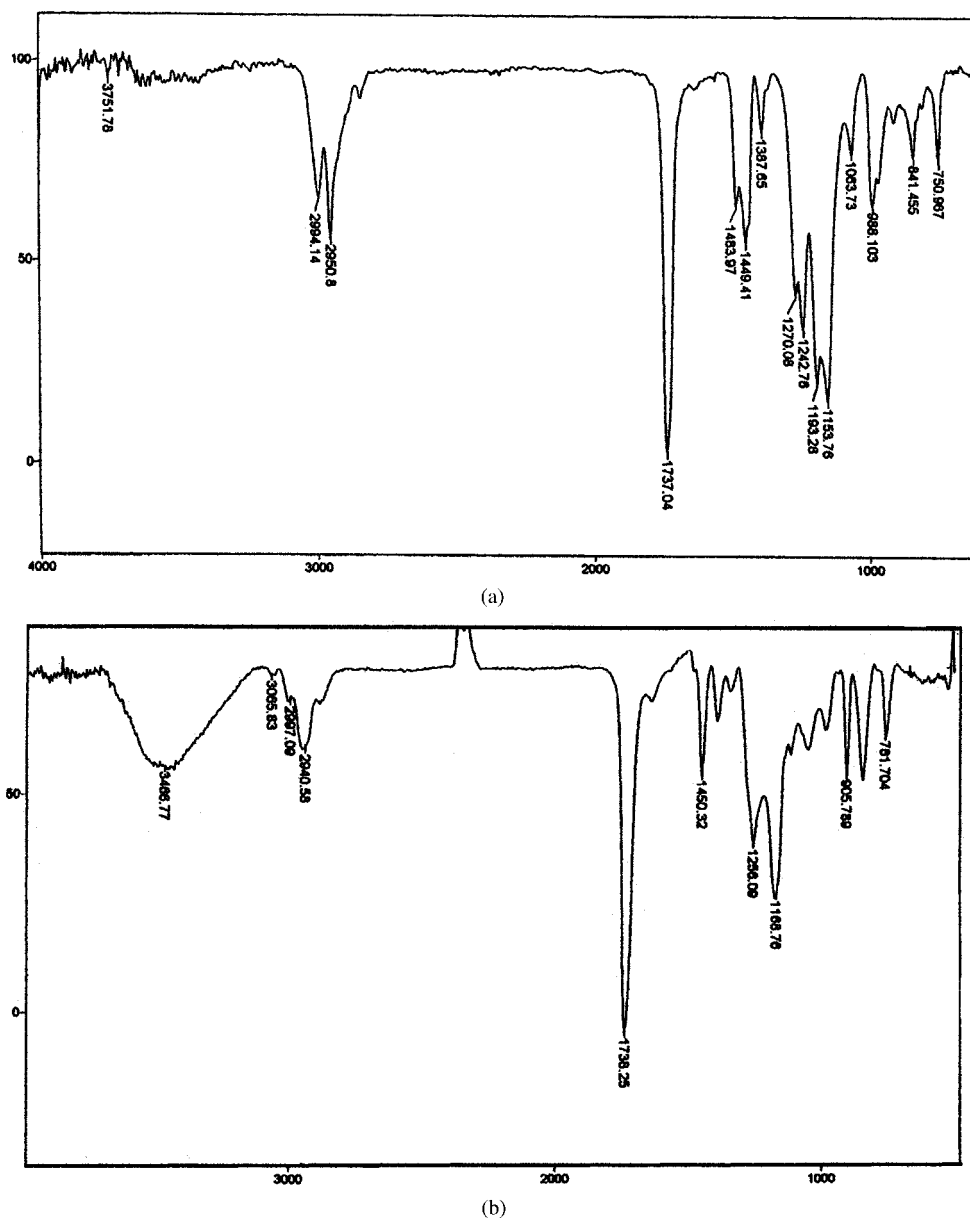


**Figure 2** FTIR spectra of (a) a PMMA coating produced at  $-0.2$  V for 15 min and (b) a PGA coating produced at  $-0.4$  V for 15 min.

desired potential and held for the required time. During the electropolymerization, nitrogen purged the air above the electrolyte. The current was supplied by a CV-27 potentiostat (Bioanalytical Systems, Inc., West Lafayette, IN) and charted by a MacLab with Chart software (ADI Instruments, Sydney, Australia). At the end of electrolysis, the working electrode was removed immediately and was rinsed in distilled water before being dried in an oven at  $50^{\circ}\text{C}$ .

#### Electropolymerizations at various times and potentials

A series of coatings were produced in the standard cell with a range of potentials and electrolysis times. The

most comprehensive survey of coatings was made from catholytes containing  $0.1\text{M}$  MMA; however, a representative series was also produced from catholytes containing  $0.1\text{M}$  GA, as shown in Table I.

#### Annealing procedure

An annealing treatment was applied to some of the coatings produced. Coatings formed from solutions containing MMA were annealed at  $200^{\circ}\text{C}$  in air for 10 min. Coatings formed from solutions containing GA were annealed at  $100^{\circ}\text{C}$  in air for 10 min. These temperatures ( $200$  and  $100^{\circ}\text{C}$ ) were chosen because they are approximately  $100^{\circ}\text{C}$  above the glass-transition

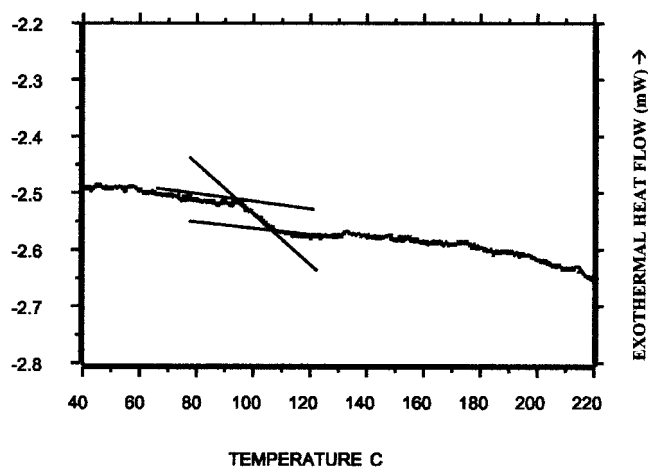


**Figure 3** DSC results of electropolymerized PMMA coating produced in the H-cell at  $-0.4$  V for 4 h.

temperature ( $T_g$ ) of poly(methyl methacrylate) (PMMA)<sup>16</sup> and poly(glycidyl acrylate) (PGA),<sup>17</sup> respectively.

#### Characterization of coatings produced in solutions containing MMA or GA

The coatings were chemically characterized by diffuse reflectance Fourier transform infrared (FTIR) spectroscopy.

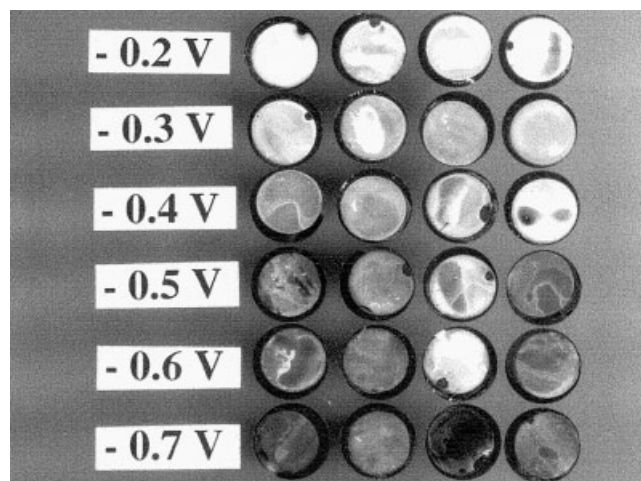


**Figure 5** Samples coated at various potentials for 15 min: catholyte 0.1M MMA in 0.01M  $K_2S_2O_8$  and 0.025M  $H_2SO_4$ . Four repeats at each potential are shown.

Spectra were obtained on a Bomem, Hartmann & Braun Fourier transform spectrometer (Quebec, Canada) and charted with Win-Bomem software (Quebec, Canada). The uniformity and coverage of the coatings were assessed visually, and the microstructures were examined by scanning electron microscopy (SEM). Thickness measurements were made on an

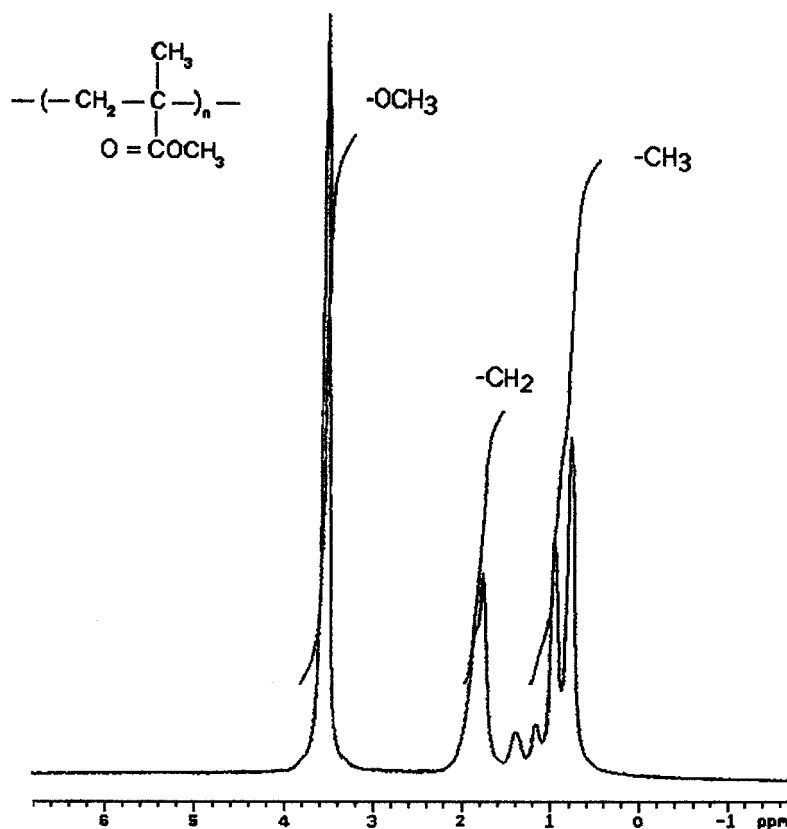


**Figure 4**  $^1H$ -NMR spectrum of electropolymerized PMMA coating produced in the H-cell at  $-0.4$  V for 4 h.

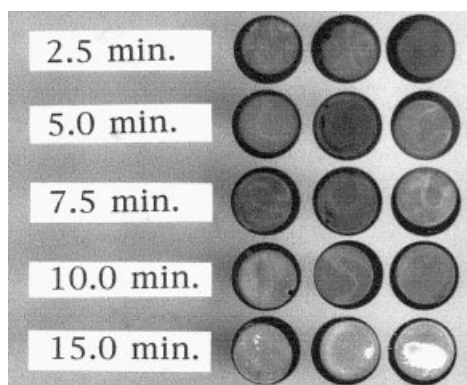


**Figure 6** Samples coated at  $-0.3$  V for various times: catholyte  $0.1M$  MMA in  $0.01M$   $K_2S_2O_8$  and  $0.025M$   $H_2SO_4$ . Three repeats at each time are shown.

Auto EL ellipsometer (Rudolph Research, Flanders, NJ) at a constant angle of incidence ( $70^\circ$ ) and wavelength ( $632.8$  nm). The refractive indices of the polymer films (both PMMA and PGA) were taken to be  $n = 1.48$  and  $k = 0$  based on the refractive index of transparent PMMA.<sup>16,18</sup> It was reasonable to assume the same refractive index for PGA as PMMA because the refractive index of polymers does not vary considerably and the effect of a small change in refractive index has been shown to be minimal on thickness calculations.<sup>19</sup> The complex refractive indices for the stainless steel oxide substrate (austenitic grade 316) was measured by ellipsometry to be  $n = 2.70$  and  $k = 3.80$ .<sup>20</sup>

#### Further characterization of coatings produced in MMA-containing solutions

Chemical characterization of coatings produced in  $0.1M$  MMA solutions was also carried out by NMR on a Varian Unity NMR facility (Springvale, Australia) at a frequency of  $300$  MHz.

Thermal characterization was carried out by DSC on Mettler TA3000 (Port Melbourne, Australia) series DSC 30 instrument. We measured  $T_g$  by scanning at a rate of  $5^\circ C/min$  from  $35$  to  $250^\circ C$  and measuring the endothermic heat change.

## RESULTS AND DISCUSSION

### Characterization of electropolymerized coatings

White opaque coatings were produced on the stainless steel cathodes from electrolytes containing either monomer. Coatings only formed during current flow, and no polymer formation within the electrolyte itself was observed during any of the experiments.

Coatings were identified by diffuse reflectance FTIR as PMMA [Fig. 2(a)] and PGA [Fig. 2(b)]. The spectrum in Figure 2(a) exhibits strong absorption peaks at

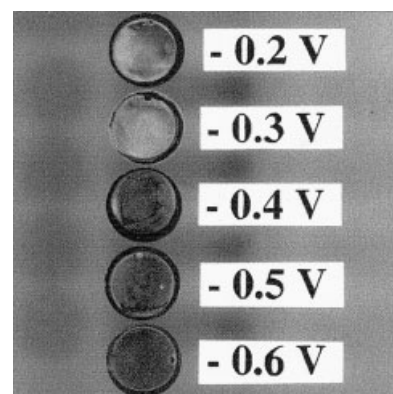


**Figure 7** Samples coated at various potentials for  $15$  min: catholyte  $0.1M$  GA in  $0.01M$   $K_2S_2O_8$  and  $0.025M$   $H_2SO_4$ .

about  $1737$   $cm^{-1}$ , corresponding to the characteristic carbonyl absorption of PMMA. No peak was observed between  $1658$  and  $1648$   $cm^{-1}$  or between  $895$  to  $885$   $cm^{-1}$ , which would indicate the presence of unreacted vinyl bonds ( $CH_2=CR$ ).

The spectrum shown in Figure 2(b) was identical to that of electropolymerized PGA formed on graphite cathodes from aqueous sulfuric acid solutions, as reported by Bell and colleagues,<sup>15</sup> confirming the product as PGA. The epoxide ring was identified by the C—H stretching at  $3065$   $cm^{-1}$  and asymmetrical ring stretching at  $905$   $cm^{-1}$ . Once again, there was an absence of any strong peaks at  $1640$ ,  $990$ , or  $811$   $cm^{-1}$  that would be attributed to unreacted vinyl bonds ( $CH_2=CHR$ ).

PMMA coatings produced over a  $4$ -h period in the H-cell at  $-0.4$  V were characterized after physical removal from the electrodes by DSC and NMR. The DSC trace (Figure 3) clearly demonstrated a reproducible change in heat flow gradient at about  $95$  to  $110^\circ C$ , indicating a reversible endothermic heat adsorption. This behavior indicated that the  $T_g$  of the polymer was between  $95$  and  $110^\circ C$ , which is typical of PMMA.<sup>16</sup>

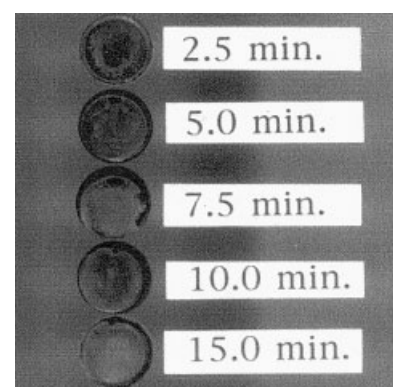


**Figure 8** Samples coated at  $-0.3$  V for various times: catholyte  $0.1M$  GA in  $0.01M$   $K_2S_2O_8$  and  $0.025M$   $H_2SO_4$ .

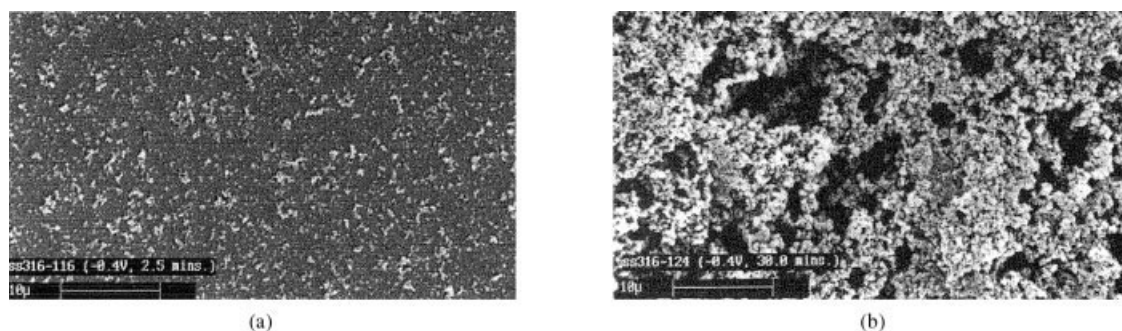


**Figure 9** Micrographs of samples treated at  $-0.3$  V for (a) 2.5 and (b) 15 min in  $0.01M$   $K_2S_2O_8$  and  $0.025M$   $H_2SO_4$  plus  $0.1M$  MMA before annealing.

$^1H$ -NMR results, shown in Figure 4, also confirmed the coating to be PMMA.<sup>21</sup> The  $-OCH_3$  resonance was clearly distinguishable at 3.6 ppm and  $-CH_2$  groups had a broader resonance between 1.5 and 2.5 ppm. However, the  $-CH_3$  groups were represented by a triad of peaks at approximately 0.8, 1.0, and 1.2 ppm, indicating the variability in tacticity of the  $-CH_3$  groups. The decreasing trend in magnitude with ppm of these three peaks indicated that the polymer was primarily syndiotactic.<sup>22</sup>

The  $T_g$  of PMMA has been reported to range from  $45^\circ C$  for fully isotactic PMMA to greater than  $130^\circ C$  for fully syndiotactic PMMA.<sup>16</sup> The DSC results, therefore, indicated that the PMMA formed had a large degree of syndiotacticity. The NMR results, shown in Figure 4, also indicated that the PMMA film was primarily syndiotactic. Free-radical polymerization of MMA always results in predominantly syndiotactic chains.<sup>18</sup> Indeed, syndiotactic chains have been reported previously for cathodic free-radical electropolymerized PMMA produced in a concentrated aqueous sulfuric acid electrolyte.<sup>11</sup>

#### Electropolymerizations at various times and potentials

The PMMA coatings were white, hazy, and opaque (Figs. 5 and 6). This haziness indicated that light was

diffused on reflectance, and this could be taken as a preliminary indication of a rough surface morphology. From visual examination, a change in coating thickness and morphology was observed as the applied potential was varied (Fig. 5). These experiments were repeated four times to ascertain the reproducibility of the coating appearance.

At low magnitudes of applied potential ( $-0.2$  V), the coatings had a very thick, opaque, white top coat, some of which peeled off during the water rinse to reveal an extremely uniform, thin, hazy under layer. As the hold potential magnitude increased, the amount and apparent thickness of this top coat decreased. At  $-0.3$  and  $-0.4$  V, very uniform homogeneous coatings were formed with a small amount of top coat. At potentials of  $-0.5$  to  $-0.7$  V, the top coat was only present as a fine powder, and the under coat progressively became less uniform in thickness and coverage.

Generally, PMMA coatings produced at  $-0.3$  and  $-0.4$  V were the most uniform; therefore, these potentials were chosen for a detailed study of polymerization time. The change in thickness and appearance of the coatings with electrolysis time can be observed in Figure 6, which shows coatings formed at  $-0.3$  V. These electropolymerization conditions were repeated at least twice, as shown, to ascertain the reproducibility

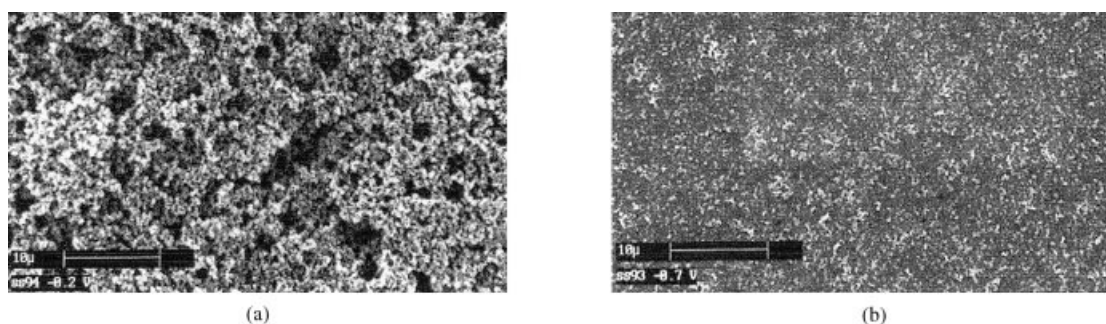


**Figure 10** Micrographs of samples treated at (a)  $-0.2$  and (b)  $-0.7$  V for 15 min in  $0.01M$   $K_2S_2O_8$  and  $0.025M$   $H_2SO_4$  plus  $0.1M$  MMA before annealing.

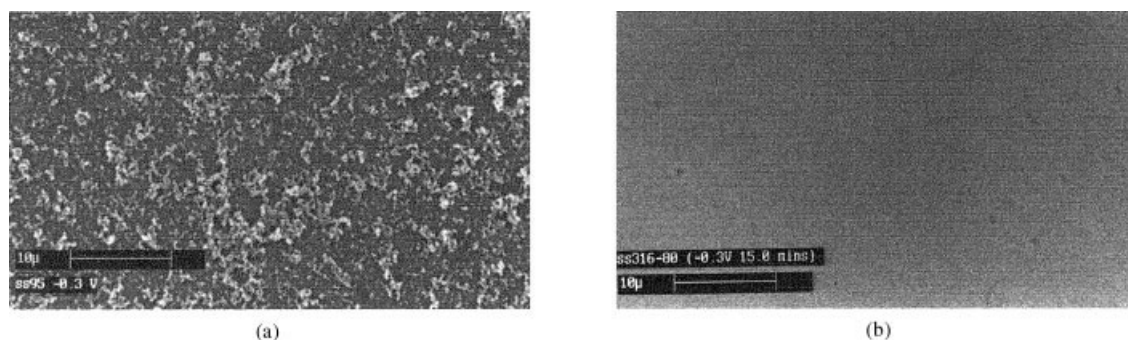


**Figure 11** Micrographs of samples treated at  $-0.3$  V for 15 min in  $0.01M$   $K_2S_2O_8$  and  $0.025M$   $H_2SO_4$  plus  $0.1M$  MMA; (a) before and (b) after annealing.

ity of the coating appearance. The coatings were relatively uniform and complete even down to the shortest electropolymerization (2.5 min).

PGA coatings produced in the same manner (Table I) also exhibited the same trends, as shown in Figures 7 and 8. However, these coatings appeared smoother, less powdery, and generally more transparent than the PMMA coatings.

#### Microstructural examination

The PMMA coatings were observed to be hazy and light diffusing; examination by SEM confirmed that this was due to a very rough surface morphology (Figs. 9 and 10). PMMA coatings produced after short electrolysis times (at  $-0.3$  V) had a smooth under layer with many small grainy deposits on top [Fig. 9(a)]. As the treatment time increased, the grainy deposits become cauliflower like and continued to increase in size until the entire surface became covered after longer times [Fig. 9(b)]. Similar cauliflower-like structures were observed when coatings of polyacrylonitrile were produced from aqueous sulfuric acid electrolytes on metallic cathodes by Teng et al.<sup>2</sup> These workers attributed the cauliflower structure to the low solubility of the polymer in the electrolyte.<sup>2</sup>

A similar transition through stages of growth was observed as a function of potential [Fig. 10(a,b)]. At

high potential magnitudes ( $-0.7$  V) when the current density was high, smooth under layers, with many small grainy deposits on top, were observed [Fig. 10(b)]. However, as the potential was lowered close to zero, the coatings formed were again more bulky and thick, through a progression of island-like growths joining together [Fig. 10(a)]. The growth of islands or globules, which conglomerated as electrolysis time increased, was also reported by Iroh et al.<sup>23</sup> for the growth of polyacrylamide films on carbon fiber cathodes from aqueous sulfuric acid electrolytes.

After the annealing treatments, the PMMA coatings became much smoother and more compact for all the coating conditions examined, as demonstrated in Figure 11(a,b) for a coating produced at  $-0.3$  V for 15 min before and after annealing.

The PGA coatings also exhibited increasing thickness with electrolysis time and decreasing potential magnitude. This was most evident from the photographs in Figures 7 and 8. However, they appeared to be more transparent, indicating that the coatings were much smoother and less porous on a microscopic scale, resulting in less scattering of the reflected light. This was indeed found to be the case when the coatings were examined by SEM (compare Figs. 11 and 12). SEM images of PGA coatings produced at  $-0.3$  V for 15 min are shown in Figures 12(a,b), before and after annealing. The coatings even before annealing

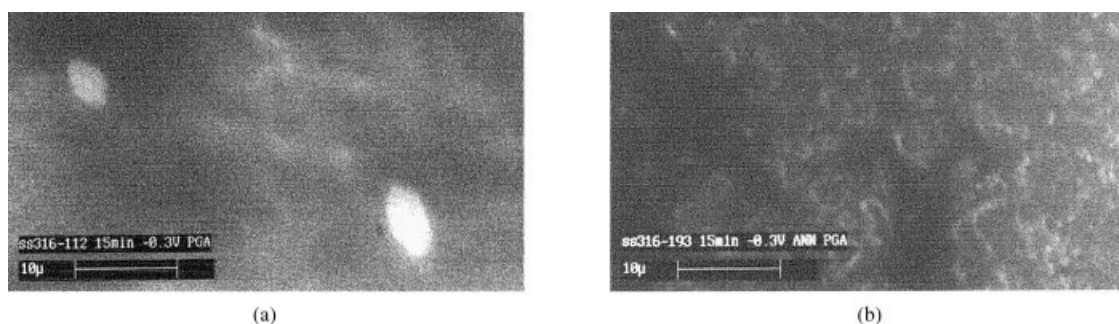


**Figure 12** Micrographs of samples treated at  $-0.3$  V for 15 min in  $0.01M$   $K_2S_2O_8$  and  $0.025M$   $H_2SO_4$  plus  $0.1M$  GA (a) before and (b) after annealing.

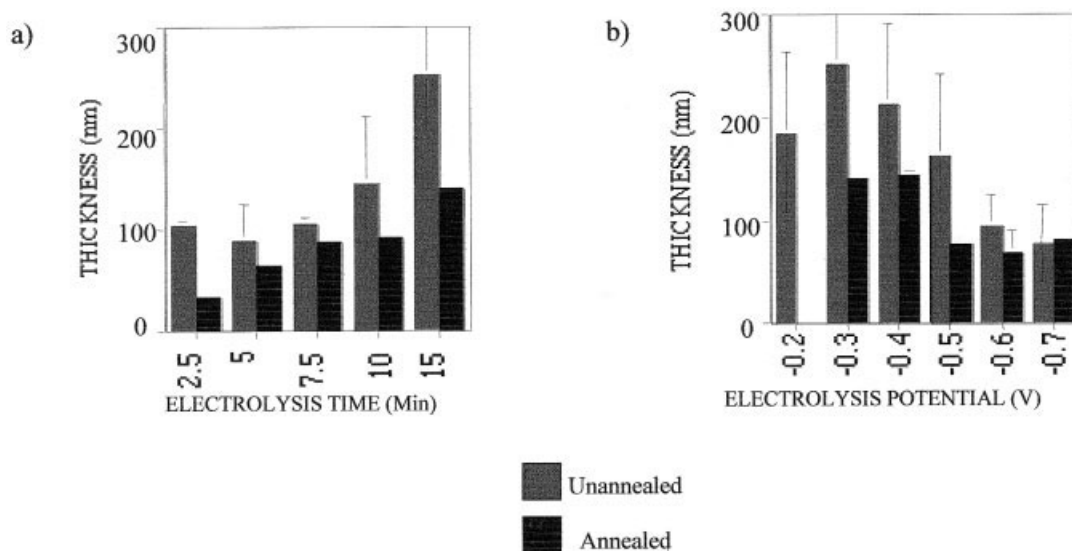


**Figure 13** Ellipsometric thickness measurements before and after annealing at 200°C for 10 min. Samples were coated in solutions of 0.1M MMA at (a)  $-0.3$  V and various times and at (b) various potentials for 15 min. (Error bars indicate one standard deviation.)

were extremely smooth and featureless, and there did not appear to be a significant change in coating morphology after annealing.

The smooth appearance of the PGA coatings could be attributed to the low  $T_g$  of this polymer (approximately 6°C),<sup>17</sup> which meant that the coatings were self-annealing at room temperature. Also the fact that the GA monomer was more soluble in the electrolyte than was MMA would cause it to form more planar, dense coatings.<sup>2</sup> Bell and Rhee<sup>13</sup> observed a honeycomb-like structure in PGA coatings formed on graphite fiber electrodes from aqueous sulfuric acid electro-

lytes. This structure was attributed to the partial crosslinking of the PGA layers.

#### Thickness measurements by ellipsometry

The PMMA and PGA coating thicknesses were quantified by ellipsometry, as shown in Figures 13 and 14. The measurements were taken before and after annealing. Generally, the thickness increased with electrolysis time and as the potential became less negative for both systems. The variability in results was much less for the PGA coatings than for the PMMA coatings.

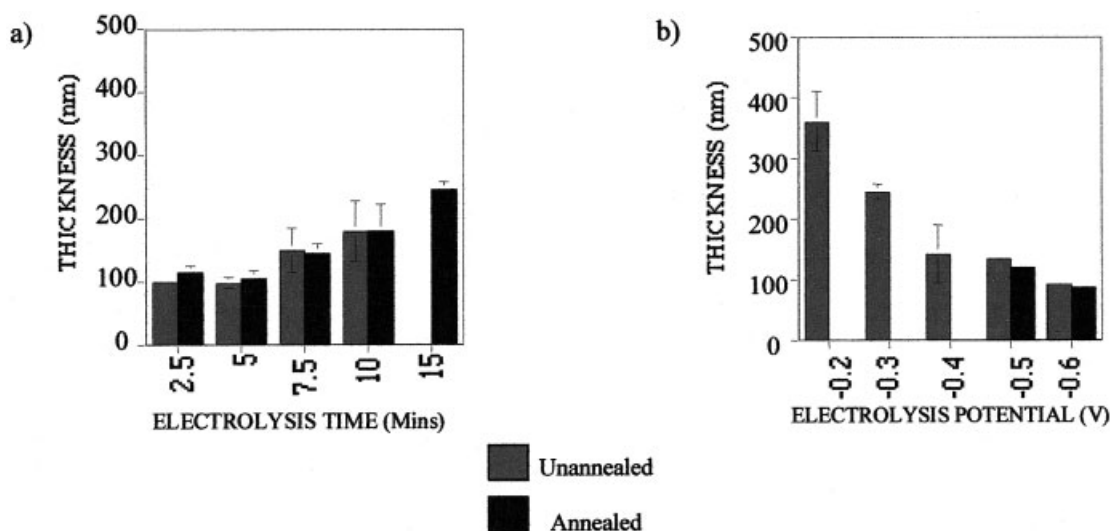


**Figure 14** Ellipsometric thickness measurements before and after annealing at 100°C for 10 min. Samples were coated in solutions of 0.1M GA at (a)  $-0.3$  V and various times and (b) various potentials for 15 min. (Error bars indicate one standard deviation.)



After very long treatment times or at potentials close to zero, the thick white top coat was too opaque for accurate thickness measurements, and these data points are missing from the charts.

### Effect of annealing

Except for the thickness of the sample treated at  $-0.2$  V in  $0.1M$  GA, the unannealed PMMA and PGA coatings were of comparable thickness. However, after annealing, the thickness of the PGA coatings did not change, whereas that of the PMMA coatings decreased considerably. This decrease in thickness was also evident visually as the PMMA coatings became more uniform and transparent. These observations indicated that the PGA coatings were substantially less porous than the PMMA coatings, which was also shown by comparison of the SEM images in Figures 11 and 12. The low  $T_g$  of PGA (approximately  $6^\circ C$ ) meant that these coatings would have undergone some viscous flow at room temperature prior to the annealing stage at  $100^\circ C$ . This would explain the smooth, transparent appearance of the coatings. The annealing treatment at  $T_g + 100^\circ C$  would, therefore, not be expected to cause a large change in thickness due to further viscous flow and decreasing porosity. The opposite effect was observed in the PMMA coatings; the porous nature of these coatings was definitely reduced by plastic flow during annealing as demonstrated in the SEM images (Fig. 11) and ellipsometry (Fig. 13).

### CONCLUSIONS

Thin, uniform films of PMMA and PGA were reproducibly formed on stainless steel cathodes from aqueous-based electrolytes. The polymer composition was confirmed by FTIR spectroscopy, and NMR spectroscopy indicated that primarily syndiotactic PMMA was produced. DSC analysis gave a  $T_g$  of approximately  $100^\circ C$ , typical of bulk PMMA. SEM analysis showed the PMMA coatings to be rough and highly porous. However, annealing for a short time at  $200^\circ C$  produced dense, smooth and optically transparent coatings. PGA coatings were smooth after deposition, and

annealing had little effect on film thickness or roughness. The thickness of the coatings was dependent on the deposition time and the applied potential with the thickness increasing with time and at less negative potentials.

The mechanism of polymerization and the effects of the ECP coating on adhesion of polymer adhesives to the stainless steel are to be reported in future publications.

### References

1. Adamcova, Z.; Dempirova, L. *Prog Org Coat* 1989, 16, 295.
2. Teng, F. S.; Mahalingham, R.; Subramanian, R. V.; Raff, R. A. V. *J Electrochem Soc* 1977, 124, 995.
3. Mengoli, G.; Musiani, M. M. *J Electrochem Soc* 1987, 134, 643C.
4. Beck, F. *Electrochim Acta* 1988, 33, 839.
5. Deng, Z.; Smyrl, W. H.; White, H. S. *J Electrochem Soc* 1989, 136, 2152.
6. Sekine, I.; Kohara, K.; Sugiyama, T.; Yuasa, M. *J Electrochem Soc* 1992, 139, 3090.
7. De Bruyne, A.; Delplancke, J.-L.; Winand, R. *J Appl Electrochem* 1995, 25, 284.
8. Subramanian, R. V.; Jakubowski, J. *J Polym Eng Sci* 1978, 18, 590.
9. Subramanian, R. V.; Jakubowski, J. J.; Williams, F. D. *J Adhes* 1978, 9, 185.
10. MacCallum, J. R.; MacKerron, D. H. *Brit Polym J* 1982, 14, 14.
11. MacCallum, J. R.; MacKerron, D. H. *Eur Polym J* 1982, 18, 717.
12. Bell, J. P.; Chang, J.; Rhee, H. W.; Joseph, R. *Polym Compos* 1987, 8, 46.
13. Bell, J. P.; Rhee, H. W. *Soc Plast Eng Annu Tech Conf* 1988, 1590.
14. Bell, J. P.; Wimolkiasak, A. S.; Rhee, H. W.; Chang, J.; Joseph, R.; Kim, W.; Scola, D. A. *J Adhes* 1995, 53, 103.
15. Kim, W.; Ahn, B.; Bell, J. P. *Polymer (Korea)* 1996, 20, 939.
16. Cholod, M. S.; Parker, H.-Y. In *Polymeric Materials Encyclopedia*; Salamone, J. C., Ed.; CRC: Boca Raton, FL, 1996.
17. Amiel, C.; Sebille, B. *J Colloid Interface Sci* 1992, 149, 181.
18. *Encyclopedia of Polymer Science and Engineering*, 2nd ed.; Kroschwitz, J. I., Ed.; Wiley: New York, 1987.
19. McCarley, R. L.; Thomas, R. E.; Irene, E. A.; Murray, R. W. *J Electrochem Soc* 1990, 137, 1485.
20. Cram, S. L. Ph.D. Thesis, University of Wollongong, Australia, 2000.
21. Pham, Q. T.; Petiand, R.; Waton, H. In *Proton and Carbon NMR Spectra of Polymers*; Penton: London, 1991.
22. Matsuzaki, K.; Uryu, T.; Asakura, T. *NMR Spectroscopy and Stereoregularity of Polymers*; Japan Scientific Societies Press: Tokyo, 1996.
23. Iroh, J. O.; Suhng, Y.; Labes, M. M. *J Appl Polym Sci* 1994, 52, 1203.